

## COMPUTATION INFORMED SELECTION OF PARAMETERS FOR PROTEIN RADICAL EPR SPECTRA SIMULATION

DIMITRI A. SVISTUNENKO<sup>a</sup>, MARY ADELUSI<sup>a</sup>, MARCUS DAWSON<sup>a</sup>,  
PAUL ROBINSON<sup>a</sup>, CATERINA BERNINI<sup>b</sup>,  
ADALGISA SINICROPI<sup>b</sup>, RICCARDO BASOSI<sup>b</sup>

**ABSTRACT.** Many important enzymatic reactions are characterised by free radical intermediates that can be detected experimentally. EPR spectroscopy can be used for monitoring formation of free radical states in enzymes. This provides vital information about the kinetic mechanism of the reactions. To uncover the molecular mechanism of the enzyme, it is necessary to know which part of the enzyme is involved in the electron transfer - where on the enzyme the radical is formed. This question is often addressed by site directed mutagenesis methods. However, the conclusions drawn from such studies are often ambiguous. A complementary method will be presented that allows radical site assignment on the basis of the EPR spectrum lineshape. Computer simulation of the lineshape requires a large number of parameters to be explicitly specified. These parameters are intimately linked to the radical conformation and its immediate microenvironment. Thus, provided the 3D structure of the enzyme is known, an experimental spectrum can be related to a specific amino acid residue in the enzyme. Unfortunately, the credibility of such approaches is weakened by the large number of input parameters in the EPR spectral simulation procedure. This difficulty can be overcome by finding relationships between these parameters. These relationships can be used for diminishing the dimension of the input parameters space. We have performed Density Functional Theory (DFT) calculations of EPR parameters of model tyrosine and tryptophan (neutral) radicals for an array of the residues' conformations, each of which is involved in a hydrogen bond of variable strength. Calculated EPR parameters are thus presented as dependences on two variables. This opens the possibility to formulate continuous functions that allow one to significantly diminish the input parameters space dimension. Successful derivation of such functions might lead to a method when an experimental EPR spectrum of a protein radical can be confidently used to pinpoint the radical location in a protein, if the protein structure is known.

**Keywords:** Tyrosine radical; Tryptophan radical; Enzymes; EPR, DFT

---

<sup>a</sup> Department of Biological Sciences, University of Essex, Wivenhoe Park, Colchester, Essex CO4 3SQ, United Kingdom, svist@essex.ac.uk

<sup>b</sup> Department of Chemistry, University of Siena, Via A. De Gasperi 53100 Siena - Italy

## INTRODUCTION

Many biological enzymes operate by employing a free radical in their mechanisms. In absolute majority of reported cases, the free radical is found either on a tyrosine (Tyr) or on a tryptophan (Trp) of polypeptide part of the enzyme. Examples of the first include: ribonucleotide reductase [1-3], prostaglandin H synthase [4,5], catalase-peroxidase [6,7], cytochrome c oxidase [8], galactose oxidase [9], glyoxal oxidase [10], dehaloperoxidase [11]. Trp radicals have been reported in cytochrome c peroxidase [12], DNA photolyase [13,14], ribonucleotide reductase [15,16], lignin peroxidase [17], ascorbate peroxidase [18], cytochrome c oxidase [19,20], versatile peroxidase [21-24].

Free radicals may also form on the proteins that are not enzymes and thus do not catalyse structural modification of molecules but rather have functions of electron transfer or small molecule (e.g. O<sub>2</sub>, NO) binding for further storage and/or transfer. Haem containing globins represent a class of such molecules, and both Tyr and Trp radicals have been shown to form on the globins when they are treated with peroxides [25-30].

The method of Electron Paramagnetic Resonance (EPR) spectroscopy allows detection of these protein bound radicals with a great degree of detail, sufficient not only to tell one radical type from another, but also to resolve differences between radicals of *the same type* if they are located at *different sites* of the protein. Thus, an EPR spectrum of a protein bound radical can be used, in principal, to figure out where on protein the radical is located.

The knowledge of radical's location is always required for understanding of the molecular mechanism of enzymes. When this knowledge is complemented with kinetic studies of the radical formation and decay, the mechanisms can be elucidated [11]. The question of radical location in proteins and enzyme is often addressed by the site directed mutagenesis method. This, however, might lead to erroneous conclusions because replacement of a residue that is not the radical's site but a site involved in the radical transfer towards the final location where the radical is observed, would affect the EPR spectrum as if the removed residue is actually the radical's host [31].

EPR spectra of radicals can be simulated on computer. Input parameters for an EPR spectra simulation program are those bits of information that are very specific to the radical type and its immediate molecular environment. The values of these parameters have to be translated into structural information, if one wants to determine a radical's location from its EPR spectrum. This is not a straightforward task since it is dozens of numerical parameters that have to be specified as an input for an EPR spectrum simulation. The Tyrosyl Radical Spectra Simulation Algorithm (TRSSA) [32] is a tool that allows diminishing the dimension of this input

space into just two truly independent input variables. These two variables are the spin density on a tyrosine's atom C1 and the rotation angle of the phenoxyl ring. To formulate a similar algorithm for Trp radicals would mean to find relationship between parameters of a Trp radical spectrum simulation and to link these relationships with as few input parameters as possible. This has not been done yet.

In order to advance in creating such an algorithm, we undertook a computational study of how EPR simulation parameters for Trp and Tyr radicals depend on two major structural factors, on the angle of rotation of the phenoxyl (in Tyr) or indole (in Trp) ring and on the strength of hydrogen bond the radicals might be engaged with. Computational works previously performed on protein radicals have demonstrated that the ring rotation angle should have a significant effect on the hyperfine interaction constants of the methylene protons, whereas a hydrogen bond should affect the  $g$ -factors, particularly the biggest, the  $g_x$  component [33-37]. In this work, we studied these effects systematically on a full range of the rings rotation (at a  $30^\circ$  interval) and on a range of hydrogen bond strengths corresponding to the range of its length of 1.55-4.2 Å

## RESULTS AND DISCUSSION

Model structures of tyrosyl and tryptophanyl radicals (Figure 1) were used to generate an array of input files for the calculation of the EPR parameters. Different rotational orientations of the rings (a full  $360^\circ$  turn at a  $30^\circ$  interval, Figure 2) were considered. For each of the ring rotation angles, a set of 6 values of distance  $d$  was considered. In total, 144 structures were used in the calculations, this is 2 radical types x 12 ring rotation orientations x 6 distances to water

Figure 3 shows dependences of the calculated principal  $g$ -factor values on the length of the hydrogen bond for tyrosyl and tryptophanyl radicals, when the ring rotation angle  $\phi$  ( $\phi_6$  for Tyr and  $\phi_4$  for Trp) was  $60^\circ$ . The  $y$  and  $z$  components of the  $g$ -factors of both Tyr and Trp radicals are practically invariant when the strength of the hydrogen bond is varied. In contrast, the  $g_x$  component of both radicals exhibits a noticeable decrease in value when the length of the H-bond becomes shorter, i.e. the bond becomes stronger. This is in agreement with previous reports [35,37-39]. Although the  $g$ -values of both radicals show similar qualitative behavior as functions on distance  $d$ , (Figures 3, A and B), the absolute spreads of the values are quite different quantitatively: if plotted on the same scale, the three curves shown in pane B will be accommodated inside the grey area in pane A.

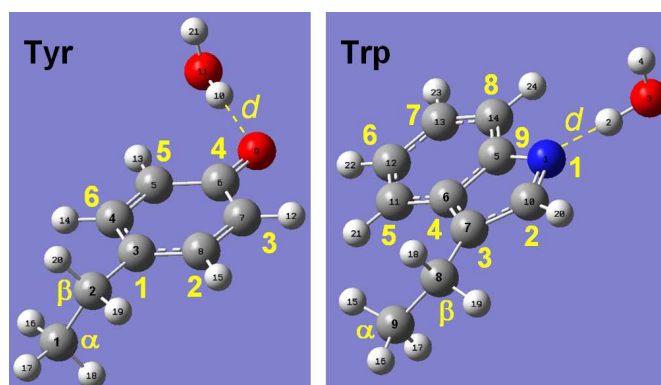


**Figure 1.** Basic Tyr and Trp model structures used in the computations. Numbers in a bigger font size and Greek letters  $\alpha$  and  $\beta$  represent conventional atom nomenclature in the two structures, whereas the smaller font size labels on the atoms stand for the internal numbering used in the computation. A water molecule is bound to the phenoxyl oxygen in the tyrosyl radical (left) and to the indole nitrogen in the tryptophanyl radical (right). The hydrogen bonds are shown as dashed lines, their lengths  $d$  were varied in the calculations. Also varied were the rotational orientations of the phenoxyl ring (around the  $C\beta$ - $C1$  bond) and indole ring (around  $C\beta$ - $C3$  bond) – dihedral angles  $\phi_6 = C\alpha$ - $C\beta$ - $C1$ - $C6$  (Tyr) and  $\phi_4 = C\alpha$ - $C\beta$ - $C3$ - $C4$  (Trp), respectively.

Dependences plotted for other rotational orientations of the phenoxyl (Tyr) and indole (Trp) rings were very similar to those shown in Figure 3. In fact, the  $g$ -factor values plotted as dependences on rotation angle, for a fixed H-bond distance, were practically horizontal lines (Figure 4). Apparently greater variations of the  $g$ -values in Trp radical are illusive: when plotted on the same scale with Tyr radicals, the three curves shown in pane B will be accommodated within the narrow grey strip in pane A (Figure 4)

Very small variations on ring rotation angle in the  $g$ -values have a  $120^\circ$  period for Trp radical, with maxima at  $\phi_4 = 60^\circ, 180^\circ$  and  $300^\circ$  (Figure 4, B) whereas the Tyr dependences have a period of  $180^\circ$  with extreme values of the three  $g$ -factors at  $\phi_6 = 0^\circ$  and  $180^\circ$  (not shown).

Principal  $g$ -values of Tyr radicals are much wider spread as compared to principal  $g$ -values in Trp radicals (Figures 3 and 4). The width of the spread behaves similar in two radicals when the strength of the hydrogen bond changes: the shorter the bond, the smaller the  $g_x$  value and therefore smaller the spread. Hydrogen bond strength has been linked before to the spin density on the  $C\gamma$  atom of tyrosyl radical, on  $C1$  [32]. It has been demonstrated that the stronger the hydrogen bond, the higher the spin density on  $C1$  [32,38,39]. This finding was new and very useful in TRSSA

since it allowed using one parameter,  $P_{C1}$ , in finding apparently independent entities required for an EPR spectrum simulation – the hyperfine interaction constants for the  $C\beta$  protons in accordance with empirical McConnell relationship [40], but also the g-factor. Now it appears that the situation with Trp radicals is quite different. Instead of a positive, it is a negative dependence between the strength of the hydrogen bond and the spin density on the  $C\gamma$  atom: the shorter the distance of the H-bond (the stronger the bond), the smaller the  $g_x$  value is and the smaller the  $P_{C3}$  is (Figure 5). This is a clear effect of the nature of the ring (indole ring instead of phenoxyl) with a different distribution of the spin density over the atoms.

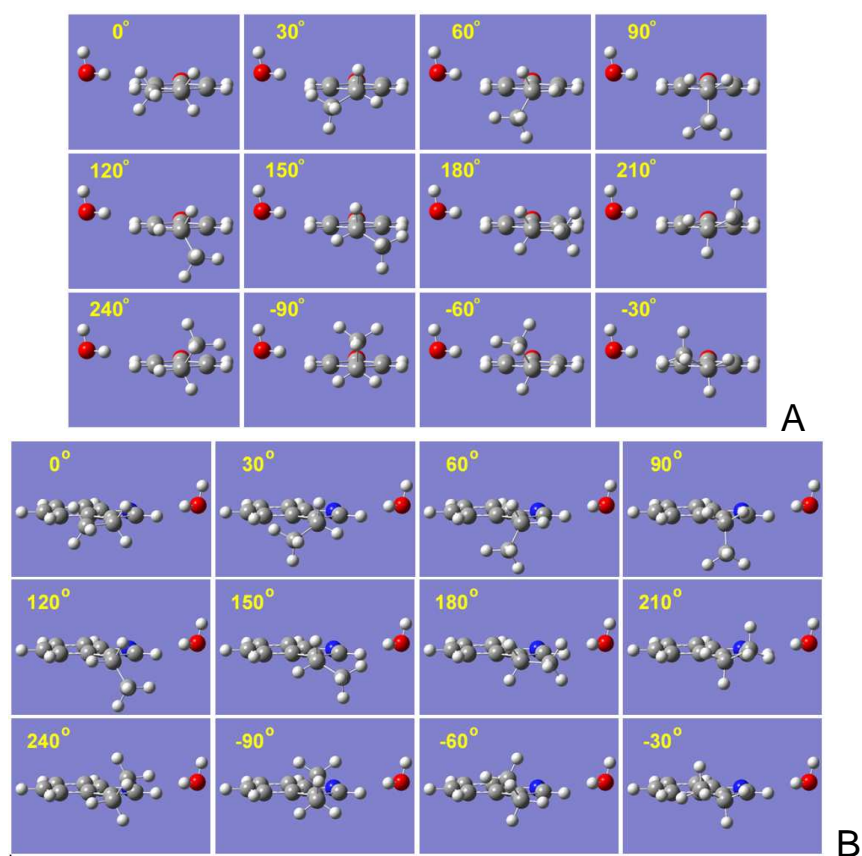


**Figure 2.** Twelve rotational conformations of the phenoxyl ring (plus water,  $d = 4.20 \text{ \AA}$ ) in tyrosyl radical (A) and twelve rotational conformations of the indole ring (plus water,  $d = 4.20 \text{ \AA}$ ) in tryptophanyl radical (B). The values of the dihedral angle  $\phi_6 = C\alpha-C\beta-C1-C6$  (in Tyr, A) and  $\phi_4 = C\alpha-C\beta-C3-C4$  (Trp, B) are shown on each pane.

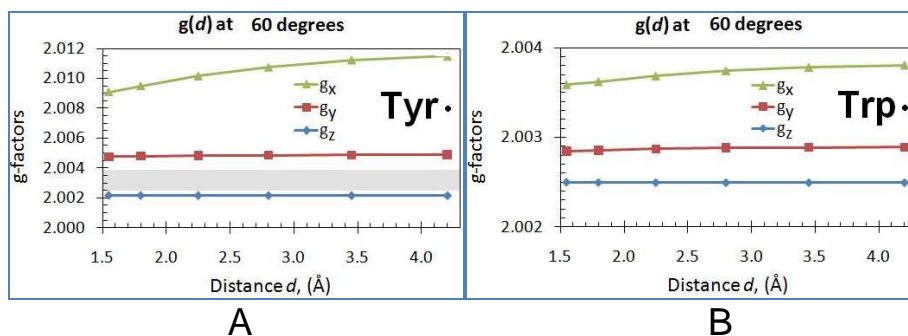


**Figure 3.** Three principal g-values of Tyr (A) and Trp radicals (B) as functions of the hydrogen bond length  $d$ . The calculations were performed for the phenoxyl ring rotation angle  $\phi_6=60^\circ$  and the indole ring rotation angle  $\phi_4=60^\circ$ . The range of g-values coloured grey in pane A corresponds to the range of the g-factor values calculated for a Trp radical presented in pane B.

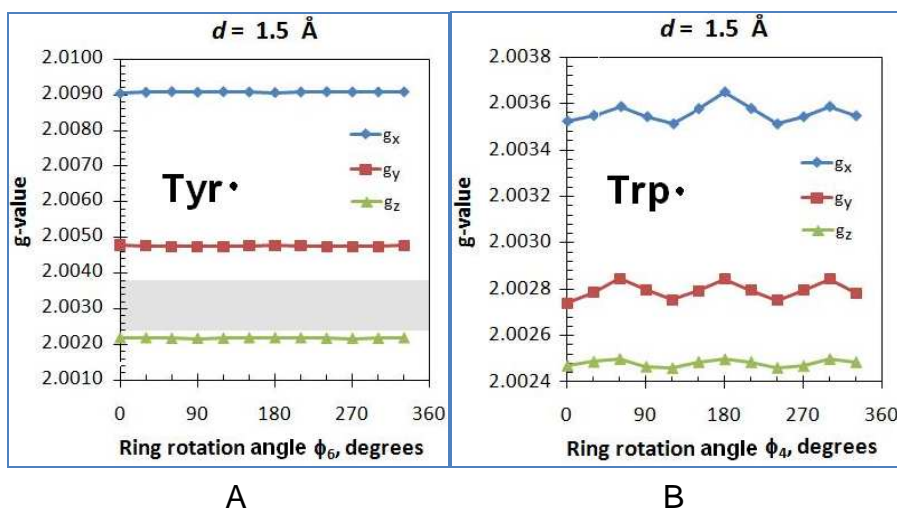


**Figure 4.** Three principal g-values of Tyr (A) and Trp radicals (B) as functions of phenoxyl or indole ring rotation angle. The data are presented for the case of the hydrogen bond length of 1.5 Å, in both radicals.

Knowing the hyperfine interaction constants for protons and nitrogens is vital for EPR spectra simulation. Generally it is accepted that a variation of the spin density distribution on a radical caused by interaction with the environment, particularly with the groups able to create H-bonds, does not affect the hyperfine interaction constants  $\blacktriangle$  very strongly. Thus the length of the H-bond is not expected to have a significant effect on these parameters. In contrast, rotation of the ring, either in Tyr or in Trp,

while having a minimal effect on the hyperfine interaction constant of the ring protons (and of the indole nitrogen in the Trp case) should have a dramatic effect on the constants of the two methylene proton of the  $\beta$  carbon ( $\beta$ -protons). Figure 6 illustrates these dependences for the  $\beta$  protons in Tyr and Trp radicals for the case of H-bond length of 1.8 Å. A periodical pattern of change of the constants is in agreement with the McConnell relationship.

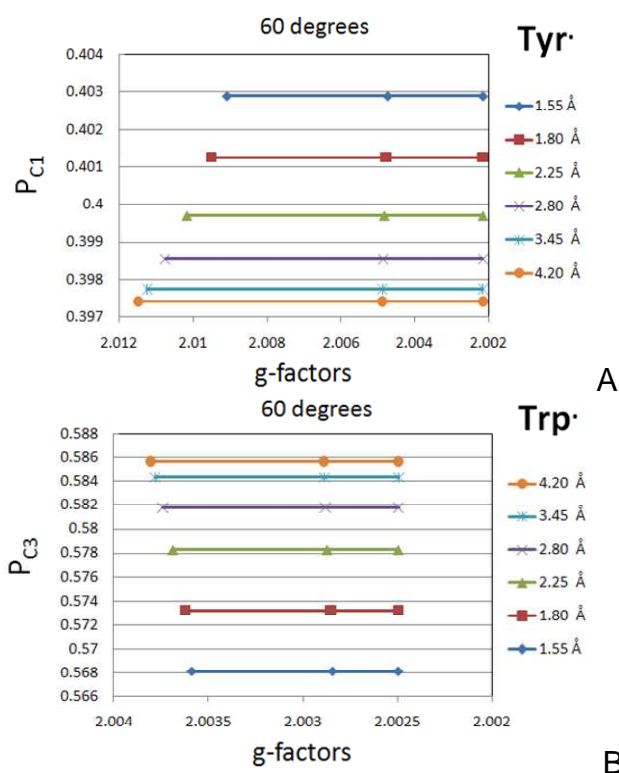


**Figure 5.** Principal g-factors of Tyr (A) and Trp (B) radicals plotted as the  $P(g)$  charts [38], i.e. when the triads of the g-factors are arranged at different heights along the vertical axis of the spin density on the  $\gamma$  carbon atoms ( $P_{C1}$  in Tyr and  $P_{C3}$  in Trp). The data points calculated for different length (strength) of the hydrogen bond illustrate strong dependences of  $g_x$  and no dependence of  $g_y$  and  $g_z$  on the spin density on the  $\gamma$  carbon atoms. The  $g_x$  value of Trp radicals increases as the spin density increases while the  $g_x$  in Tyr decreases.

For each proton, two of the three components of the  $\mathbf{A}$ -tensor are close to each other whereas the third component ( $cc$ ) is greater than either of the two. That makes the symmetry of the  $\mathbf{A}$ -tensor of the methylene  $\beta$  protons axial and of a slightly *prolate* shape (cigar like, in contrast to the *oblate*, which is a disk like shape).

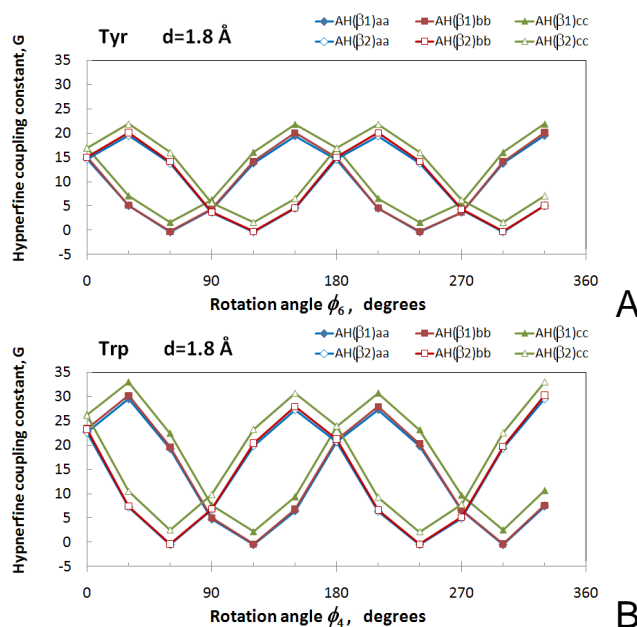


**Figure 6.** Hyperfine interaction constants for the  $\beta$  (methylene) protons in Tyr (A) and Trp (B) radicals. Dependences on the rings rotation angles  $\phi_6$  (Tyr) and  $\phi_4$  (Trp) are presented for the case of the H-bond length of 1.8 Å. Three principal components of the hyperfine interaction tensor  $\mathbf{A}$  are presented for each proton, corresponding to the directions aa, bb and cc. The  $\beta_1$  and  $\beta_2$  protons are atoms H19 and H20, respectively, in Tyr and atoms H18 and H19, respectively, in Trp (see Figures 1 and 2)

As expected for the range of the H-bond lengths studied, the methylene protons' hyperfine interaction constants depend weakly on the H-bond strength (Figure 7). It has been shown, however, at least for tryptophan radicals, that as the H-bond length becomes very short and a proton transfer becomes possible (which would turn a neutral tryptophanyl radical into a cation radical) the spin density on C3 and, correspondingly, the  $\mathbf{A}$ -values for methylene protons decrease significantly [37]. When comparing these dependences calculated for the two types of radical (with  $d \geq 1.55$  Å), when one of the protons is in the ring plane and thus having principal  $\mathbf{A}$ -values close to zero, we would notice that the constants for the other proton in Tyr are slightly increasing as the H-bond strength becomes stronger. An immediate explanation that comes to mind is that this is because the spin density on C1 is increasing (Figure 5, A) and this causes an increase in the  $\mathbf{A}$ -values in accordance with the McConnell relationship. We, however have to admit that the mechanism is likely to be more complex than that, since the increase of the  $P_{C1}$  in the range of H-bond



distances studied is  $\sim 1.7\%$  (Figure 5, A) whereas the increase of the average  $\Delta$ -value for  $\beta_2$  proton is about 8% (Figure 7, A). This fact highlights once again the conclusion [38] that McConnell relationship is approximate and that the coefficients  $B'$  and  $B''$  in it are not particularly constant when the relationship is applied to different cases.

The  $\Delta$ -value dependences on shortening of the H-bond in Trp radical are not as clear monotonous curves as in the Tyr case, likely because the  $P_{C3}$  is decreasing in Trp radical, in contrast to  $P_{C1}$  in Tyr radical (Figure 5).

## CONCLUSIONS

A full analysis of the EPR parameters of the 144 structures of Tyr and Trp radicals is under way and will be published elsewhere. The principal g-factor values and hyperfine interaction constants for H and N atoms will be reported for an array of ring orientations and hydrogen bond strengths (12 rotation angles  $\times$  6 H-bond distances), for each radical. This two dimensional array of data points for each EPR parameter will create a basis of analytical formulation of a continuous surface that could be used to find the parameter for any combination of rotation angle and H-bond strength. Derivation of such functions should lead to a new method of assigning of an experimental EPR spectrum of a Tyr or Trp radical to a specific Tyr or Trp site on the protein, with a high degree of confidence.

## EXPERIMENTAL SECTION

A technical background describing relationship between empirical (simulation derived) radical parameters and those calculated by the computational chemistry methods from the crystal structure of the radicals is given elsewhere [38]. The structures as shown in Figure 1 but with variable angle of the rings rotation and with variable distance towards the water molecules were analysed. The *Gaussian03* software package [41] was used for both the optimisations of the structures and the calculation of the EPR parameters, both at the B3LYP/6-31G\* level of theory. During the optimization, the atom coordinates that define the rings rotation angles and the distances to the water molecule were kept frozen. Single point calculations were then performed for finding g-factor values, spin densities and hyperfine interaction constants.

## ACKNOWLEDGMENTS

DAS acknowledges a COST Action P15 travel grant to visit the University of Siena. CB, AS and RB acknowledge the CINECA 2011 Award HP10C9HMGL, for high performance computing resources and support.

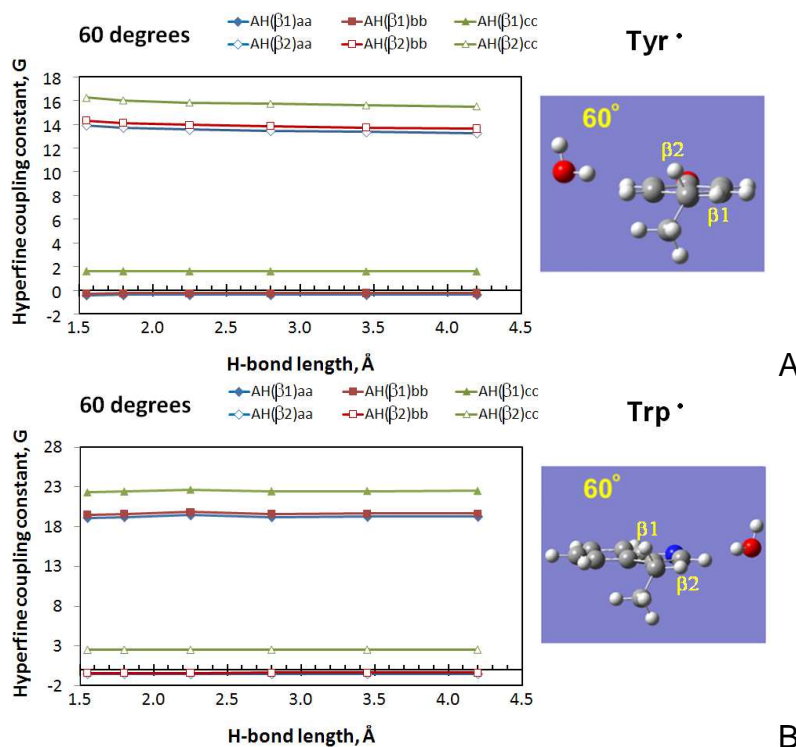


**Figure 7.** Hyperfine interaction constants for the  $\beta$  (methylene) protons in Tyr (A) and Trp (B) radicals. Dependences on the hydrogen bond length are presented for the case of the phenoxyl (in Tyr) and indole (in Trp) rings rotation angle of  $60^\circ$ . As in Figure 6, three principal components of the hyperfine interaction tensors are presented; the nomenclature of the  $\beta 1$  and  $\beta 2$  protons in each case is as given in Figure 6 caption.

## REFERENCES

1. M. Sahlin; A. Gräslund; A. Ehrenberg, B.-M. Sjöberg, *Journal of Biological Chemistry*, **1982**, 257, 366-369.
2. P. Reichard, A. Ehrenberg, *Science*, **1983**, 221, 514-519.
3. P. Allard; A. L. Barra; K. K. Andersson; P. P. Schmidt; M. Atta, A. Gräslund, *Journal of The American Chemical Society*, **1996**, 118, 895-896.
4. L. C. Hsi; C. W. Hoganson; G. T. Babcock, W. L. Smith, *Biochemical and Biophysical Research Communications*, **1994**, 202, 1592-1598.
5. P. Dorlet; S. A. Seibold; G. T. Babcock; G. J. Gerfen; W. L. Smith; A. L. Tsai, S. Un, *Biochemistry*, **2002**, 41, 6107-6114.

6. S. Chouchane; S. Girotto; S. Yu, R. S. Magliozzo, *Journal of Biological Chemistry*, **2002**, 277, 42633-42638.
7. X. Zhao; S. Girotto; S. Yu, R. S. Magliozzo, *Journal of Biological Chemistry*, **2004**, 279, 7606-7612.
8. D. A. Svistunenko; M. T. Wilson, C. E. Cooper, *Biochimica et Biophysica Acta*, **2004**, 1655, 372-380.
9. G. T. Babcock; M. K. El-Deeb; P. O. Sandusky; M. M. Whittaker, J. W. Whittaker, *Journal of The American Chemical Society*, **1992**, 114, 3727-3734.
10. M. M. Whittaker; P. J. Kersten; N. Nakamura; J. Sandersloehr; E. S. Schweizer, J. W. Whittaker, *Journal of Biological Chemistry*, **1996**, 271, 681-687.
11. M. K. Thompson; S. Franzen; R. A. Ghiladi; B. J. Reeder, D. A. Svistunenko, *Journal of The American Chemical Society*, **2010**, 132, 17501-17510.
12. M. Sivaraja; D. B. Goodin; M. Smith, B. M. Hoffman, *Science*, **1989**, 245, 738-740.
13. S. T. Kim; A. Sancar; C. Essenmacher, G. T. Babcock, *Proceedings of the National Academy of Sciences U.S.A.*, **1993**, 90, 8023-8027.
14. C. Aubert; M. H. Vos; P. Mathis; A. P. Eker, K. Brettel, *Nature*, **2000**, 405, 586-590.
15. M. Sahlin; G. Lassmann; S. Pötsch; A. Slaby; B. M. Sjöberg, A. Gräslund, *Journal of Biological Chemistry*, **1994**, 269, 11699-11702.
16. F. Lendzian; M. Sahlin; F. MacMillan; R. Bittl; R. Fiege; S. Pötsch; B.-M. Sjöberg; A. Gräslund; W. Lubitz, G. Lassmann, *Journal of The American Chemical Society*, **1996**, 118, 8111-8120.
17. W. Blodig; A. T. Smith; K. Winterhalter, K. Piontek, *Archives of Biochemistry and Biophysics*, **1999**, 370, 86-92.
18. A. N. Hiner; J. I. Martinez; M. B. Arnao; M. Acosta; D. D. Turner; E. Lloyd Raven, J. N. Rodriguez-Lopez, *European Journal of Biochemistry*, **2001**, 268, 3091-8.
19. F. G. Wiertz; O. M. Richter; A. V. Cherepanov; F. MacMillan; B. Ludwig, S. de Vries, *FEBS Letters*, **2004**, 575, 127-30.
20. F. G. Wiertz; O. M. Richter; B. Ludwig, S. de Vries, *Journal of Biological Chemistry*, **2007**, 282, 31580-91.
21. R. Pogni; M. C. Baratto; S. Giansanti; C. Teutloff; J. Verdin; B. Valderrama; F. Lendzian; W. Lubitz; R. Vazquez-Duhalt, R. Basosi, *Biochemistry*, **2005**, 44, 4267-4274.
22. R. Pogni; M. C. Baratto; C. Teutloff; S. Giansanti; F. J. Ruiz-Duenas; T. Choinowski; K. Piontek; A. T. Martinez; F. Lendzian, R. Basosi, *Journal of Biological Chemistry*, **2006**, 281, 9517-9526.
23. R. Pogni; C. Teutloff; F. Lendzian, R. Basosi, *Applied Magnetic Resonance*, **2007**, 31, 509-526.
24. F. J. Ruiz-Duenas; R. Pogni; M. Morales; S. Giansanti; M. J. Mate; A. Romero; M. J. Martinez; R. Basosi, A. T. Martinez, *Journal of Biological Chemistry*, **2009**, 284, 7986-7994.
25. D. Tew, P. R. Ortiz de Montellano, *Journal of Biological Chemistry*, **1988**, 263, 17880-17886.
26. M. J. Davies, A. Puppo, *Biochemical Journal*, **1992**, 281, 197-201.
27. J. A. DeGray; M. R. Gunther; R. Tschirret-Guth; P. R. Ortiz de Montellano, R. P. Mason, *Journal of Biological Chemistry*, **1997**, 272, 2359-2362.

28. D. A. Svistunenko, *Biochimica et Biophysica Acta*, **2005**, 1707, 127-155.
29. D. A. Svistunenko; B. J. Reeder; M. M. Wankasi; R.-L. Silaghi-Dumitrescu; C. E. Cooper; S. Rinaldo; F. Cutruzzolà, M. T. Wilson, *Dalton Transactions*, **2007**, 840-850.
31. D. A. Svistunenko; J. 30. B. J. Reeder; M. Grey; R. L. Silaghi-Dumitrescu; D. A. Svistunenko; L. Bulow; C. E. Cooper, M. T. Wilson, *Journal of Biological Chemistry*, **2008**, 283, 30780-30787.
- Dunne; M. Fryer; P. Nicholls; B. J. Reeder; M. T. Wilson; M. G. Bigotti; F. Cutruzzolà, C. E. Cooper, *Biophysical Journal*, **2002**, 83, 2845-2855.
32. D. A. Svistunenko, C. E. Cooper, *Biophysical Journal*, **2004**, 87, 582-595.
33. S. Un; M. Atta; M. Fontecave, A. W. Rutherford, *Journal of The American Chemical Society*, **1995**, 117, 10713-10719.
34. F. Himø; A. Gräslund, L. A. Eriksson, *Biophysical Journal*, **1997**, 72, 1556-1567.
35. S. Un, *Magnetic Resonance Chemistry*, **2005**, 43, S229-S236.
36. M. Brynda, R. D. Britt, *Research In Chemical Intermediates*, **2007**, 33, 863-883.
37. C. Bernini; R. Pogni; F. J. Ruiz-Duenas; A. T. Martinez; R. Basosi, A. Sinicropi, *Physical Chemistry Chemical Physics*, **2011**, 13, 5078-5098.
38. D. A. Svistunenko, G. A. Jones, *Physical Chemistry Chemical Physics*, **2009**, 11, 6600-6613.
39. C. Bernini; A. Sinicropi; R. Basosi, R. Pogni, *Applied Magnetic Resonance*, **2010**, 37, 279-288.
40. H. M. McConnell, D. B. Cheshunt, *Journal of Chemical Physics*, **1958**, 28, 107-117.
41. M. J. Frisch, G. W. Trucks, H. B. Schlegel, G. E. Scuseria, M. A. Robb, J. R. Cheeseman, J. Montgomery, J. A., T. Vreven, K. N. Kudin, J. C. Burant, J. M. Millam, S. S. Iyengar, J. Tomasi, V. Barone, B. Mennucci, M. Cossi, G. Scalmani, N. Rega, G. A. Petersson, H. Nakatsuji, M. Hada, M. Ehara, K. Toyota, R. Fukuda, J. Hasegawa, M. Ishida, T. Nakajima, Y. Honda, O. Kitao, H. Nakai, M. Klene, X. Li, J. E. Knox, H. P. Hratchian, J. B. Cross, V. Bakken, C. Adamo, J. Jaramillo, R. Gomperts, R. E. Stratmann, O. Yazyev, A. J. Austin, R. Cammi, C. Pomelli, J. W. Ochterski, P. Y. Ayala, K. Morokuma, G. A. Voth, P. Salvador, J. J. Dannenberg, V. G. Zakrzewski, S. Dapprich, A. D. Daniels, M. C. Strain, O. Farkas, D. K. Malick, A. D. Rabuck, K. Raghavachari, J. B. Foresman, J. V. Ortiz, Q. Cui, A. G. Baboul, S. Clifford, J. Cioslowski, B. B. Stefanov, G. Liu, A. Liashenko, P. Piskorz, I. Komaromi, R. L. Martin, D. J. Fox, T. Keith, M. A. Al-Laham, C. Y. Peng, A. Nanayakkara, M. Challacombe, P. M. W. Gill, B. Johnson, W. Chen, M. W. Wong, C. Gonzalez, J. A. Pople 2004 *Gaussian 03*. 2004, Gaussian, Inc.: Wallingford CT.